

UNCLASSIFIED

AD NUMBER

AD818298

LIMITATION CHANGES

TO:

Approved for public release; distribution is unlimited.

FROM:

Distribution authorized to U.S. Gov't. agencies and their contractors; Critical Technology; JUL 1967. Other requests shall be referred to Air Force Technical Application Center, Washington, DC. This document contains export-controlled technical data.

AUTHORITY

usaf ltr, 28 feb 1972

THIS PAGE IS UNCLASSIFIED

AD818298

**SEISMIC DATA LABORATORY
QUARTERLY TECHNICAL
SUMMARY REPORT**

17 JULY 1967

Prepared for

**AIR FORCE TECHNICAL APPLICATIONS CENTER
Washington, D. C.**

By

TELEDYNE, INC.

Under

Project VELA UNIFORM



Sponsored By

ADVANCED RESEARCH PROJECTS AGENCY

Nuclear Test Detection Office

ARPA Order No. 624

SEISMIC DATA LABORATORY
QUARTERLY TECHNICAL
SUMMARY REPORT

PAGES NOT FILMED ARE BLANK

17 July 1967

AFTAC Project No.: VELA T/6702
Project Title: Seismic Data Laboratory
ARPA Order No.: 624
ARPA Program Code No.: 5810

Name of Contractor: TELEDYNE, INC.
Contract No.: F 33657-67-C-1313
Date of Contract: 2 March 1967
Amount of Contract: \$ 1,735,617
Contract Expiration Date: 1 March 1968
Project Manager: William C. Dean
(703) 836-7644

P.O. Box 334, Alexandria, Virginia

AVAILABILITY

This document is subject to special export controls and each transmittal to foreign governments or foreign national may be made only with prior approval of Chief, AFTAC.

The work reported herein was supported by the Advanced Research Projects Agency, Nuclear Test Detection Office, under Project VELA-UNIFORM and accomplished under the technical direction of the Air Force Technical Applications Center under Contract F 33657-67-C-1313.

Neither the Advanced Research Projects Agency nor the Air Force Technical Applications Center will be responsible for information contained herein which may have been supplied by other organizations or contractors, and this document is subject to later revision as may be necessary.

TABLE OF CONTENTS

	Page No.
I. <u>INTRODUCTION</u>	1
II. <u>WORK COMPLETED</u>	1
A. <u>Multiple Coherence of Seismic Noise</u>	1
1. Short-Period Noise Field at LASA	3
2. Long-Period Noise Field at LASA	4
3. Short-Period Noise at three Vertical Arrays - UBSO, GV-TX, AP-OK	5
4. Short-Period Noise at UBSO and TFSO	5
B. <u>LASA Analyses</u>	6
1. The Detection Threshold at The Montana LASA	6
2. Distribution of Short-Period P-Phase Ampli- tudes over LASA	6
3. Correlation of Amplitude Anomalies at LASA	7
C. <u>Radiation of Seismic Waves from The BILBY Explosion</u>	8
D. <u>Synthesis of Additive Ambient Seismic Noise With A Gaussian Markov Model</u>	9
E. <u>Principal Component Analysis of Seismic Data</u>	10
F. <u>Eigenvalues and Eigenvectors of Spectral Density Matrices</u>	11
G. <u>Shot and Earthquake Analyses</u>	11
III. <u>SUPPORT AND SERVICE TASKS</u>	12
A. <u>VELA-UNIFORM Data Services</u>	12
B. <u>Data Library</u>	12
C. <u>Data Compression</u>	15
D. <u>Automated Bulletin Process</u>	15

Appendix A - Organizations Receiving SDL Data Services

LIST OF ILLUSTRATIONS

Figure No.

Follows Page No.

1.	Multiple coherences versus frequency for both inter & intrasubarray noise recorded at LASA on 29 October 1965	3
2.	Multiple Coherence vs. Frequency for two LP-Z Samples from LASA.	4
3.	Multiple Coherence versus frequency for a UBSO sample recorded in December 1966. The upper diagram uses the surface instrument as output; the lower uses the deepest instrument as output.	5
4.	Multiple Coherence vs. Frequency with 2-8 Inputs for two noise samples recorded at UBSO, January 1967	5
5.	Multiple Coherences vs. Frequency with 2-9 Inputs for two noise samples recorded at TFSO, January 1967	5
6.	P-P Amplitudes of an Earthquake As Recorded at all LASA SPZ Seismometers	7
7.	P-P Amplitudes of An Earthquake As Recorded At Each Subarray.	7

Table No.

1.	Event Magnitudes at LASA	6
2	Seismic Data From Three Nuclear Explosions	11

I. INTRODUCTION

This quarterly technical summary report covers the work performed during the period April through June 1967. Work previously completed or currently in progress is mentioned only as it relates to analyses completed during this reporting period.

Analyses completed, for which results have been reported, are discussed in Section II under descriptive headings. Section III contains a discussion of the support and service tasks performed for in-house projects and for other VELA-UNIFORM participants. Appendix A is a listing of those organizations receiving SDL data services during this period.

II. WORK COMPLETED

A. Multiple Coherence of Seismic Noise

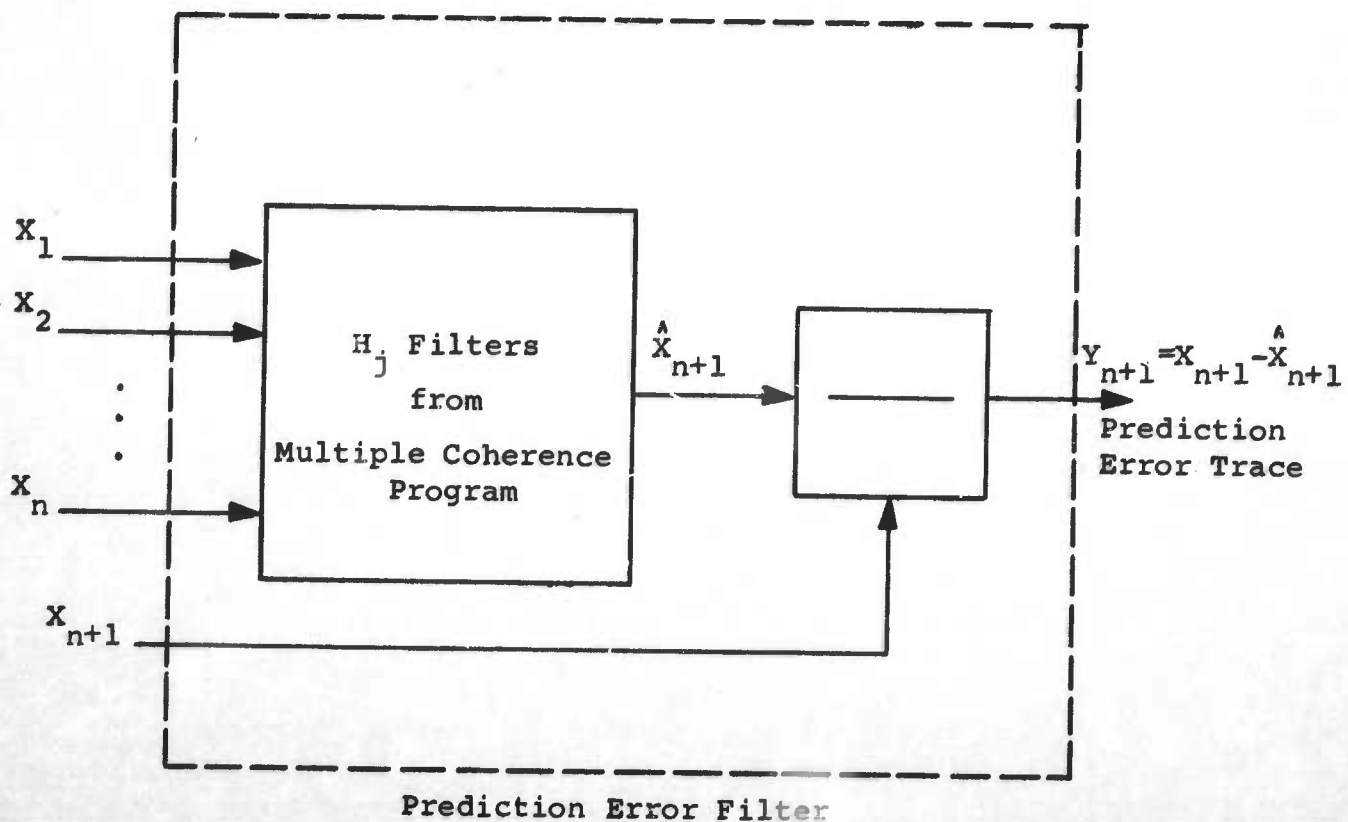
Most basic data processing techniques for signal enhancement or identification depend upon the structure of the noise within the seismic array. If some of the coherent noise is due to site characteristics such as consistently coherent noises from particular directions, then techniques using multiple coherence will help to isolate these consistent linear relations. Many optimum filters for estimating the signal take account of these linear relations implicitly by weighting with the inverse of the spectral noise matrix. However, one cannot tell whether the coherent noise involved is due to noise generating events which cannot be predicted or controlled. Thus, the filters must be recalculated over a period of noise recording immediately prior to the arrival of each single signal. Part of the coherent noise generated within the array may be due to various causal factors for a particular array. If so, we can learn something about these factors by examining the linear relations between the various array elements. A potential benefit here is that a consistent linear model relating the different sub-elements would eliminate the need for computing a different set of filter coefficients for each event.

The multiple coherence function can indicate how many seismometer outputs in an array are necessary to properly determine the seismic noise field. If there are n independent seismic noise components, then the multiple coherence function would be unity when $(n + 1)$ st seismometers are placed in an array to measure seismic noise records. If part of the background is composed of incoherent noise, then the multiple coherence function would indicate the percentage of coherent noise present and the number of seismometers necessary to define this coherent noise. The filter relations determined by the

multiple coherence computations can then be used in array summation to bring the noise into destructive interference.

This analysis does not guarantee that such optimum processing is possible. For example, if the noise and signal propagation characteristics across the array are identical, no velocity filtering scheme can be expected to separate the two even though the multiple coherence might be unity.

The multiple coherence function is the frequency domain equivalent of the prediction error filter in time. If n input seismic traces predict the $(n + 1)$ st trace in an array completely, then the multiple coherence will be unity and a prediction error filter could be used to exactly predict this $(n + 1)$ st output. In fact, linear filter relations derived by the multiple coherence program produce an estimate of the $(n + 1)$ st trace which, when subtracted from the actual $(n + 1)$ st trace, given a prediction error trace. Thus the combination of the filter derived in the multiple coherence program and the subtraction operation produces a prediction error filter as shown in the following diagram:



This multiple coherence function was used to estimate the degree of predictability for the following:

- short-period noise field at LASA
- long-period noise field at LASA
- short-period noise field at vertical arrays - UBSO, GV-TX and AP-OK
- short-period noise field at UBSO and TFSO

1. Short-Period Noise Field at LASA

The multiple coherences of short-period data for both within the subarray (intrasubarray) and between subarrays (intersubarray) were computed, as shown in Figure 1. It was concluded from this study that:

- a. Intersubarray noise at LASA shows a low multiple coherence over all frequencies, even with 9 input channels.
- b. Even the closest subarrays at LASA show little coherency.
- c. Intrasubarray noise at LASA shows a high multiple coherence for frequencies of 1 cps and lower when 7 or more inputs are used. However, the 7th, 8th, and 9th inputs are only $\frac{1}{2}$ km away from the output trace. When the closest inputs are 2 km away from the output, the multiple coherences are significantly less than .8 for all but microseismic frequencies.
- d. The digital programs will show high coherence and multiple coherence when present, e. g., LONGSHOT event has high multiple coherence over subarrays. An Andreanof earthquake, a weaker event than LONGSHOT, shows multiple coherences between those of LONGSHOT and noise - only cases.
- e. Low multiple coherence is not due to insufficient lags. The programs have sufficient resolution to handle noise propagation with velocity, 1 km/sec and less.
- f. Power spectra from the seismometers at 500 feet agree with those at 200 feet only out to 1.2 cps. Beyond this frequency the power spectra density of the deeper seismometers continue to fall, while the power spectra densities from the shallow seismometers rise.
- g. The multiple coherence using shallow seismometers as inputs trying to match the deeper seismometer as output falls rapidly beyond 1.2 cps.
- h. The intrasubarray multiple coherence using shallow seismometers are both inputs and output is approximately the same

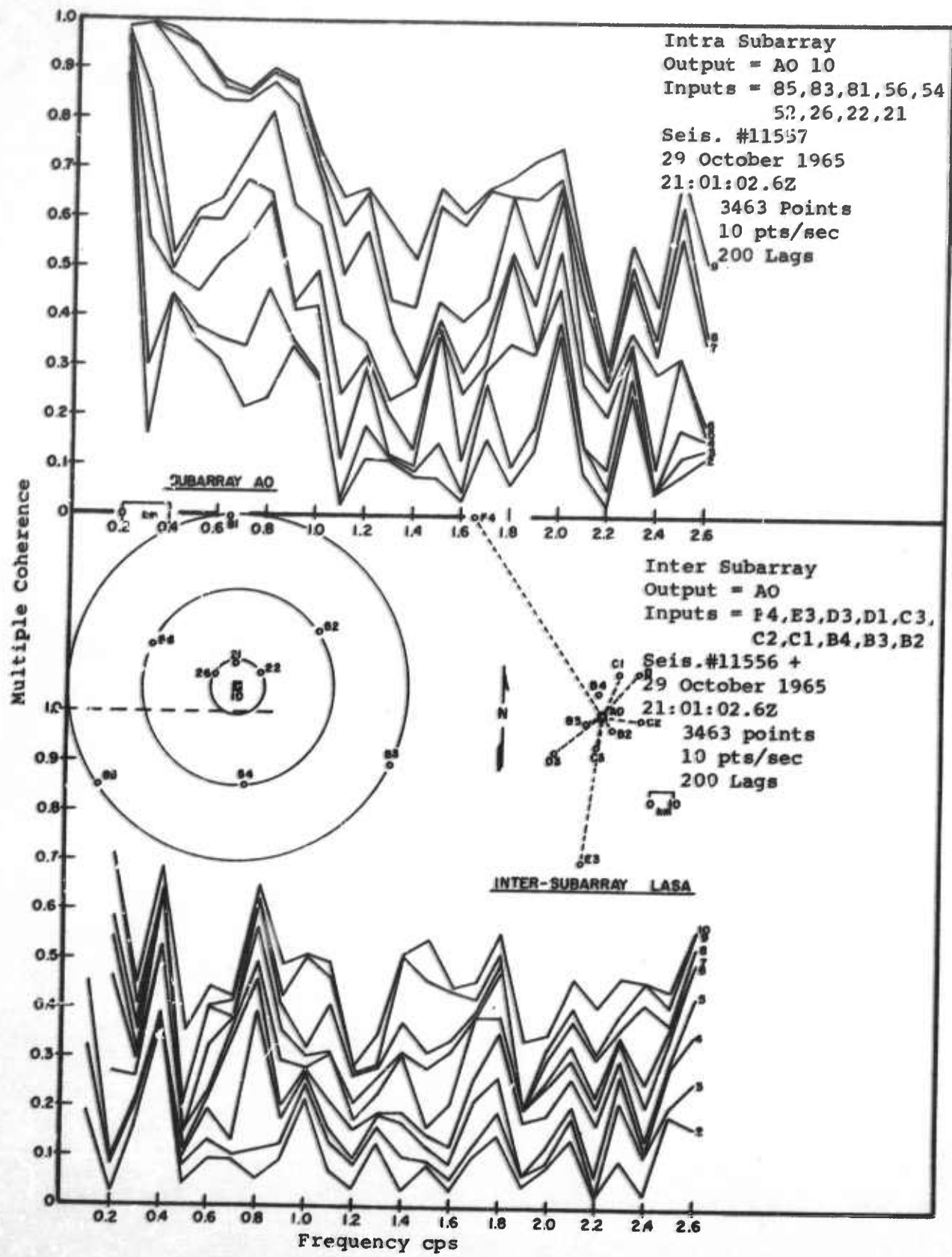


Figure 1. Multiple coherences versus frequency for both inter and intrasubarray noise recorded at LASA on 29 October 1965.

as for intrasubarray multiple coherences which uses the trace from the 500-foot hole as output. This result is obtained in spite of a striking difference in the power spectra of the shallow and deep seismograms.

- i. The intersubarray multiple coherence indicates that the expected noise reduction from a prediction error filter is about 1 db over the fitting interval and about 0 db outside the fitting interval.

2. Long-Period Noise Field at LASA

The multiple coherence was computed of long period LASA data for the vertical components only. These seismometers are located at the center of each subarray. Consequently, all computations are intersubarray coherences with a maximum of 21 channels available. Figure 2 shows the multiple coherences versus frequency for two of the three time samples tested. Results led to the following conclusions:

- a. Multiple coherences for all long-period samples increase significantly with an increase in the number of input channels.
- b. From mid-range of the long-period pass band toward the microseismic frequencies (7-20 seconds period) the multiple coherences are greater than .65 with 8 or 9 input channels.
- c. The expected noise reduction from a prediction error filter in the fitting interval is as much as 9 db at 16 seconds period. The noise reduction outside the fitting interval at 16 seconds period is from 3-4 db.
- d. Over the 7-20 second period range, the expected noise reduction from a prediction error filter in the fitting interval is about 4 db. Over the same 7-20 second period range an average of 1 db is obtained outside the fitting interval.
- e. The db improvement figures given above were computed when only 7 input channels were available. We estimate that the db improvement both within and outside the fitting interval would be increased with more input channels.
- f. Over the 7-20 second period range the multiple coherences for all samples tested are quite similar to each other up to 6 or 7 input channels. Since the 9 channels available for one sample showed a significant increase in the multiple coherence over the 6 and 7 channel examples, we conclude that at least 9 input channels are necessary to adequately model the long period noise at LASA.

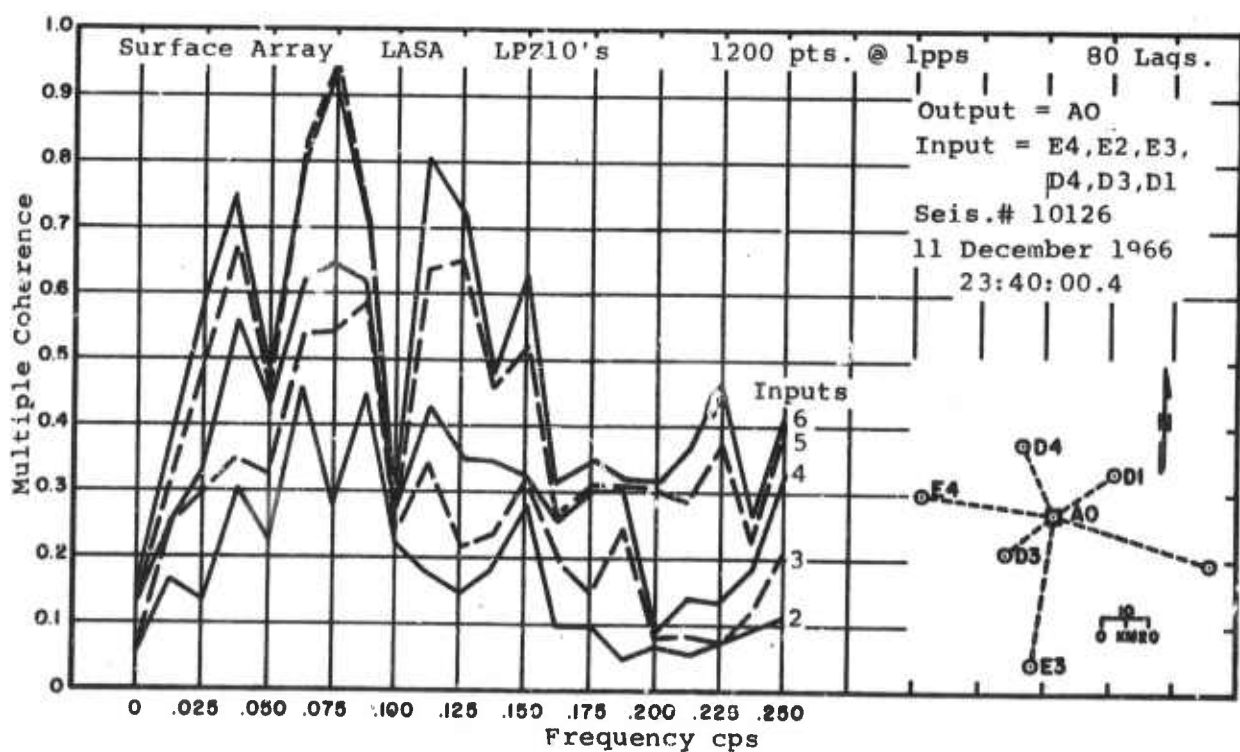
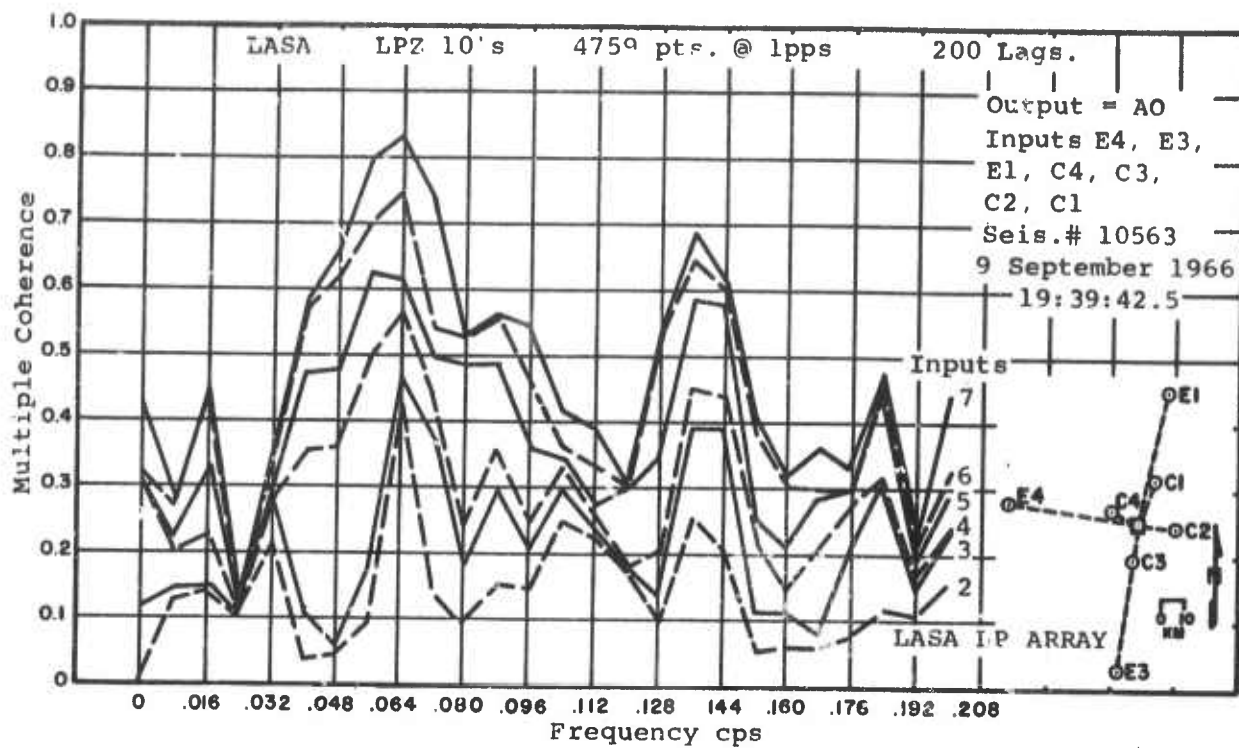


Figure 2. Multiple Coherence vs. Frequency for two LP-Z Samples from LASA.

3. Short-Period Noise at Three Vertical Arrays - UBSO, GV-TX, AP-OK

The multiple coherence of short-period vertical component data from the three vertical arrays was computed. Figure 3 shows multiple coherence versus frequency for the two output cases. The upper diagram shows multiple coherence with a surface instrument as output. The lower diagram shows the multiple coherence with the deepest instrument as output. It was concluded that:

- a. The multiple coherence properties of the noise at the three vertical arrays with similar geometries are similar. At all three sites the downhole channels correlate with each other better than with the surface channel. At all three sites the coherence between downhole seismometers decreases markedly as their separation increases.
- b. When the deep trace is the output and all seismometers are added as inputs, the multiple coherence is highest at GV-TX. In fact it is greater than .85 for all frequencies from .1 to 2.5 cps. For the AP-OK and UBSO wells the multiple coherence varies between .6 to .9 for most frequencies greater than .5 cps..
- c. All three sites show a significant 2 cps component in the noise spectra for most of the examples tested. The multiple coherence of this 2 cps component is high but not appreciably higher than other noise frequencies above the microseismic band. Even the surface trace correlates well with the down-hole traces for the 2 cps component.
- d. The noise at AP-OK appears to be more stationary than noise at the surface arrays. For three successive $3\frac{1}{2}$ minute samples the expected noise reduction from a prediction error filter applied in the fitting interval was 16 to 20 db over the microseismic band and between 2 and 7 db for frequencies greater than 0.5 cps. Outside the fitting interval the expected noise reduction was within 2 db of these values.

4. Short-Period Noise at UBSO and TFSO

The multiple coherences were computed from arrays of short-period vertical component seismometers. Figures 4 and 5 show the multiple coherence versus frequency for two noise samples recorded at UBSO and TFSO respectively. It was concluded that:

- a. The multiple coherence of the noise at UBSO and TFSO short-period, vertical component arrays is high (greater than 0.9) over the microseismic frequency.
- b. The decay of the multiple coherence of the noise with increasing frequency is faster at TFSO than at UBSO and faster at UBSO than at LASA subarrays.

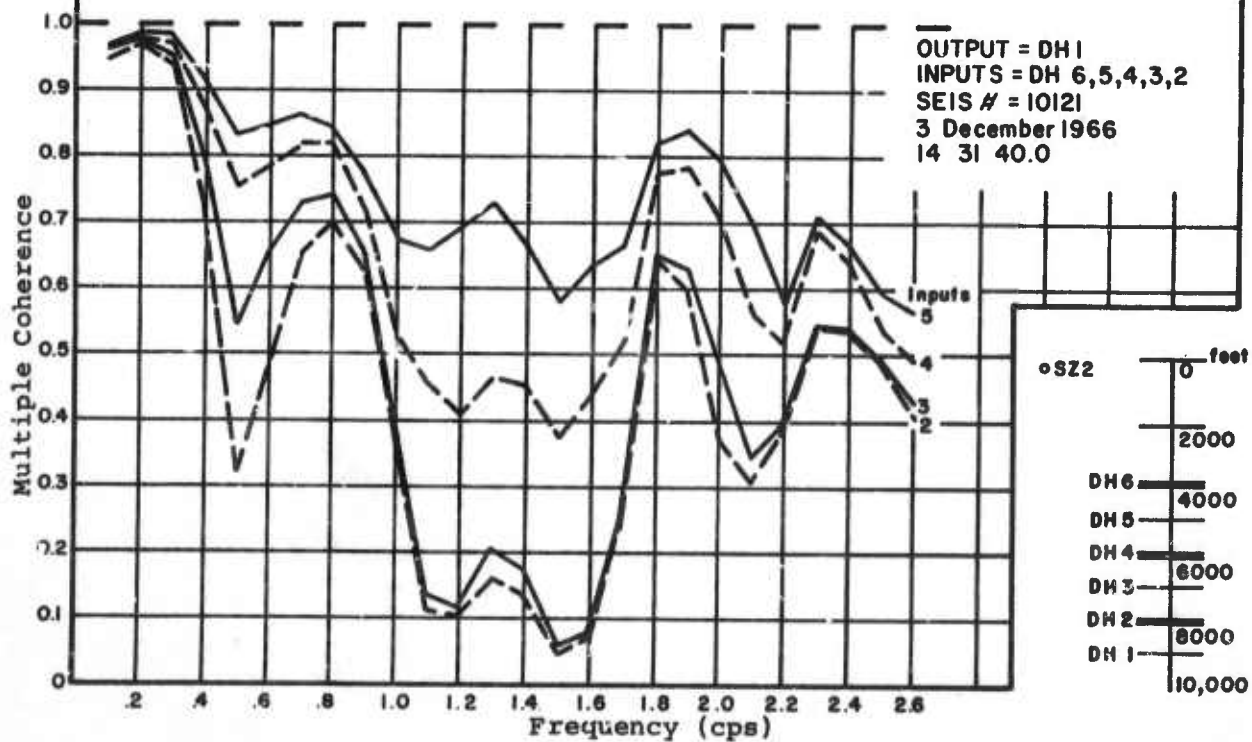
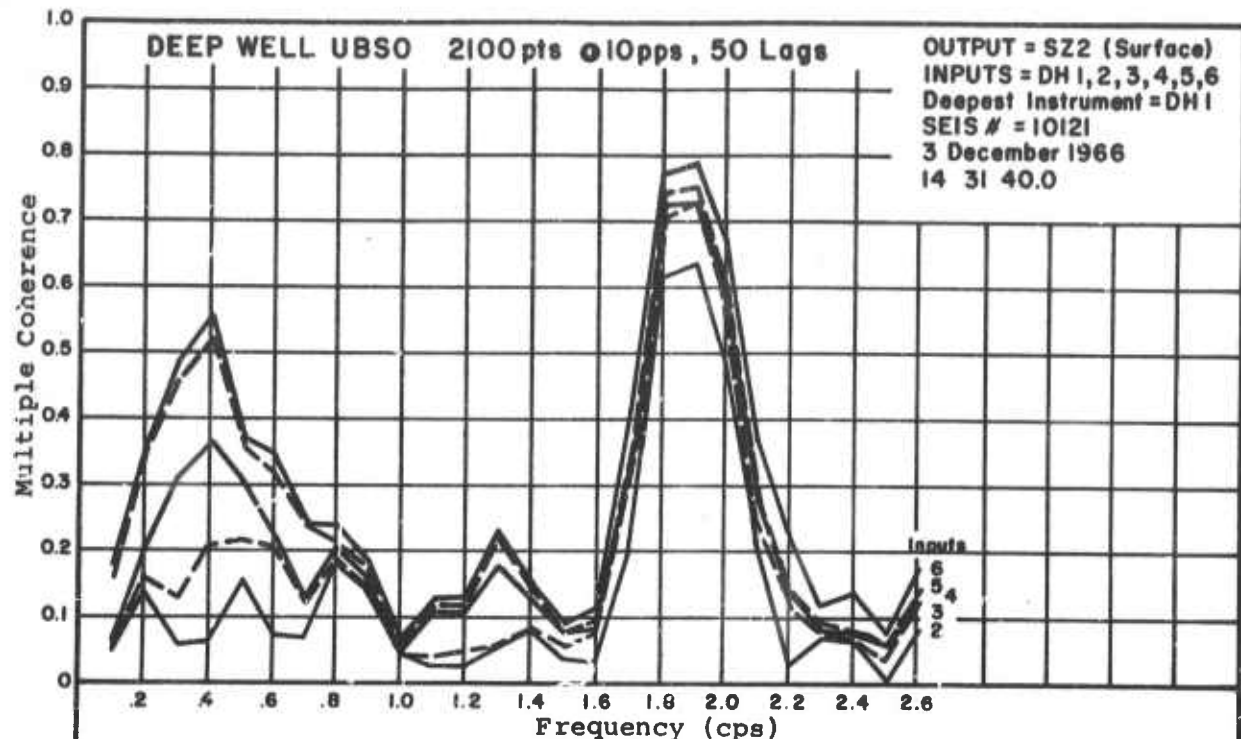


Figure 3. Multiple coherence versus frequency for a UBSO sample recorded in December 1966. The upper diagram uses the surface instrument as output; the lower uses the deepest instrument as output.

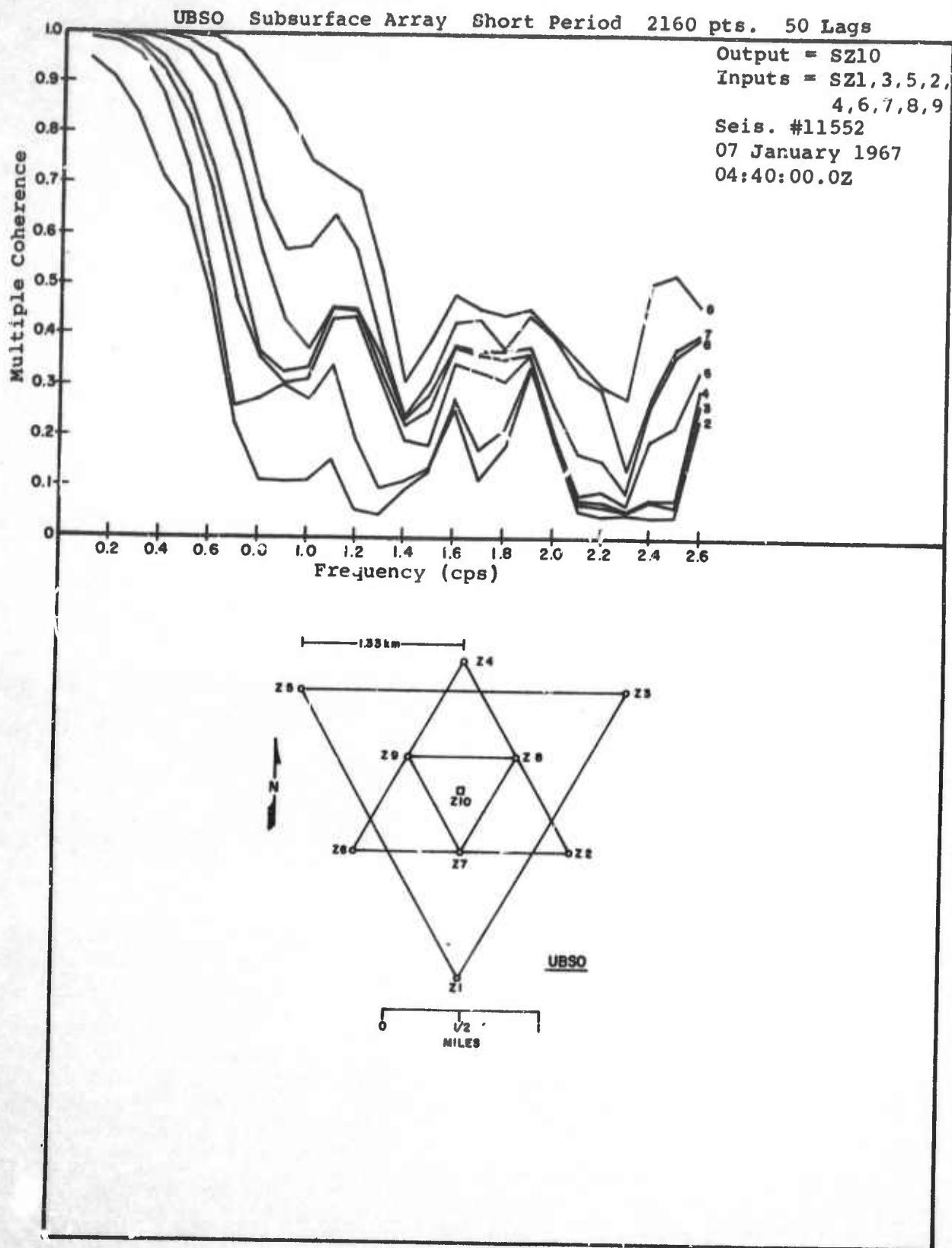


Figure 4. Multiple Coherence vs. Frequency with 2-8 Inputs
for two noise samples recorded at UBSO, January 1967.

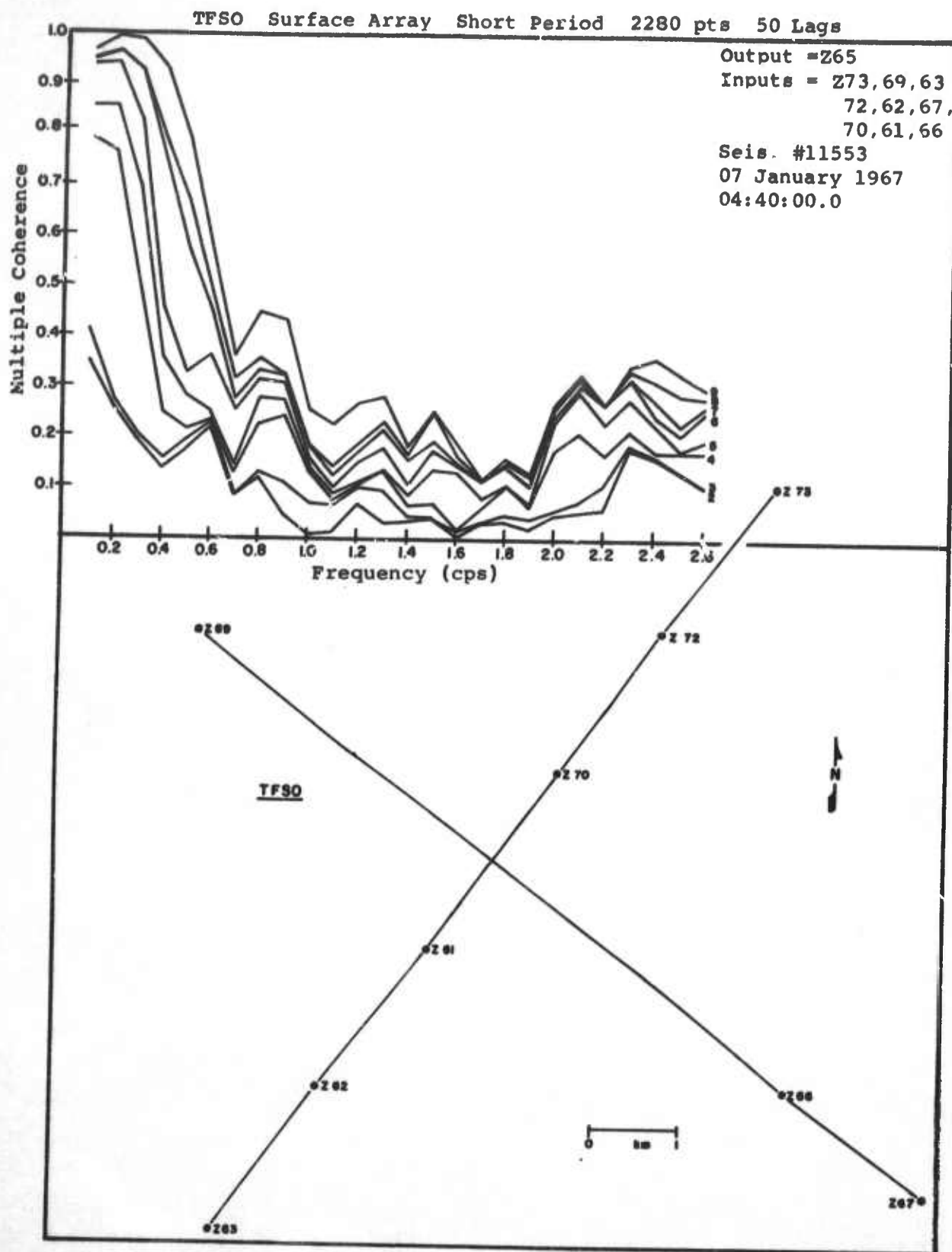


Figure 5. Multiple Coherences vs. Frequency with 2-9 Inputs
for two noise samples recorded at TFSO, January 1967.

- c. The noise has a low multiple coherence (less than .4) with up to 9 inputs at UBSO and TFSO for frequencies greater than 1.5 cps. Thus the noise is largely incoherent over the upper part of the signal band at UBSO and TFSO.
- d. The noise at UBSO and TFSO over adjacent time samples is stationary only over the microseismic frequency band.

B. LASA Analysis

1. The Detection Threshold at The Montana LASA

As part of the continuing study to evaluate the Montana LASA, an analysis was made to determine a detection threshold at the LASA for events originating at teleseismic distances. Any such magnitude value is highly generalized since it depends not only on the epicentral distance and azimuth, depth of the hypo-center, and the source mechanism, but also on the precision of the beamforming process and the type of prefiltering used. Moreover, it is undoubtedly a function of the recording period. By this is meant that the nighttime noise level is lower than that recorded during the daylight hours, and detection threshold estimates will be lower than that obtained from a similar set of events recorded during the day. For this study, the basic procedure was to use LASA beamformed outputs from 56 events recorded at night to compute event magnitudes and corresponding threshold values.

Table 1 summarizes the results of this analysis and shows C&GS magnitude, LASA Magnitude, LASA threshold magnitude, and averages for the 56 events analyzed to date. These data illustrate two important points. First, the average C&GS magnitude differs from the average LASA magnitude by less than 0.1, even though LASA computations were based on data taken from beamformed output traces. Second, the Montana LASA should be able to detect a mixture of shallow and deep events of average magnitude 3.6 as a result of the beamforming process. For bombs and shallow quakes, the threshold would be 0.1 higher because of the correction factor for deep foci. For daytime recordings we estimate that it would be an additional 0.1-0.2 higher because of higher noise levels. Obviously, this magnitude, 3.6, is highly generalized since it is a function of several parameters, which include epicentral distance and azimuth, source mechanism, beamforming precision, and type of bandpass filter used.

2. Distribution of Short-Period P-Phase Amplitudes Over LASA

In the following, the distribution of the peak to peak (p-p) amplitudes for several events at LASA will be considered and it will be shown that this data approaches a log-normal distribution.

Plotting the p-p amplitudes of all SPZ seismometers at LASA for a single event against frequency of occurrence yields a graph which seems to have no familiar probability distribution. Figure 6, which shows

EVENT	$m_{C \& GS}$	m_1	m_0		EVENT	$m_{C \& GS}$	m_1	m_0
1.	4.1	4.3	3.4		29.	3.9	4.1	3.3
2.	4.3	4.4	3.5		30.	5.0	5.0	3.6
3.	4.3	4.3	3.4		31.	4.9	4.8	3.2
4.	5.7	5.7	3.4		32.	5.2	5.6	3.5
5.	5.2	5.0	3.8		33.	5.1	5.2	3.6
6.	5.1	5.4	3.6		34.	4.1	4.2	3.2
7.	5.1	4.9	3.7		35.	4.4	4.6	3.6
8.	4.7	4.6	3.7		36.	5.6	5.3	3.9
9.	4.7	5.1	3.6		37.	4.8	5.0	3.6
10.	4.9	4.6	3.5		38.	6.0	5.5	3.7
11.	5.0	4.8	3.6		39.	4.6	4.9	3.8
12.	5.1	5.0	3.7		40.	6.3	6.1	3.9
13.	5.2	5.6	3.8		41.	4.8	5.3	3.7
14.	4.5	4.8	3.8		42.	5.8	5.8	3.8
15.	*3.9	3.9	3.7		43.	6.3	6.3	3.9
16.	3.9	4.1	3.3		44.	*5.8	6.2	3.8
17.	4.9	5.0	3.2		45.	4.9	4.9	3.9
18.	4.8	4.7	3.2		46.	5.5	5.6	3.8
19.	4.9	4.7	3.4		47.	5.7	5.5	3.8
20.	5.3	5.4	3.3		48.	4.8	4.6	3.8
21.	4.3	4.6	3.4		49.	5.0	5.1	3.7
22.	5.0	5.5	3.5		50.	5.2	5.6	3.9
23.	4.5	4.3	3.5		51.	4.8	4.8	3.3
24.	4.9	4.7	3.5		52.	*3.9	4.3	3.9
25.	4.3	4.5	3.7		53.	*4.8	5.3	4.0
26.	4.6	3.9	3.4		54.	*3.7	3.9	3.3
27.	3.8	4.3	3.3		55.	*3.3	3.4	3.4
28.	4.6	4.9	3.7		56.	*4.0	-	-
AVERAGES						4.91	4.96	3.6

*NON C & GS MAGNITUDE (Not included in average)

Table 1. Event Magnitudes at LASA

the p-p amplitudes of an earthquake is a typical graph of this type. However, if the p-p amplitudes that are associated with a given subarray are inspected, a pattern emerges. There is generally a modal clustering with a short tail toward decreasing values and a long tail toward increasing values suggesting that the data may come from a log-normal distribution (Figure 7).

It was evident that some subarrays exhibit a higher degree of sensitivity for events from one source region than for events from another. These consistencies indicate that the individual subarrays are biased in a certain sense due to the travel path of the source signal. Since the elements in each subarray are closely spaced, in comparison to the distance separating subarray centers, it was found that the individual subarray preference from all of the subarrays could be eliminated by considering each subarray as a sampling of the population of the p-p amplitudes and standardizing each sampling in the usual sense, i.e., if a subarray has a $N(m,s)$ distribution describing the behavior of the observations x , then the linear transformation will give the standardized distribution $N(0,1)$.

$$y = \frac{m-x}{s}$$

By applying this transformation to all subarrays over every event, all subarrays and all events can be pooled and then the properties of the entire pool can be investigated. If the assumption that the logarithms of the p-p amplitudes in each subarray are normally distributed is valid, then the pooled distribution will also be normally distributed.

One hundred and fifty seven seismograms of eight events yielded 3,925 usable amplitude records which were used to test this hypothesis. Results showed a definite tendency toward normality of the data. Plots of the data gave a visual indication regarding the normality of the data. Statistically, the distribution was χ^2 -tested for normality with the result that at the 5% level of significance the sample distribution is consistent with the hypothesis that the parent distribution is normal.

3. Correlation of Amplitude Anomalies at LASA

Certain consistencies have been shown to exist among the anomalies of short period teleseismic P-phase amplitudes when those anomalies are grouped according to geographical regions. The purpose of this study was to present evidence that the source path strongly influences the observed amplitude anomalies.

Eight earthquakes from the same geographical area, viz., the Fiji Islands, were selected for this investigation. All eight events

The distribution of the P-P amplitudes follows no familial pattern. Bimodality appears present in this event (cf. Fig. 16) but this characteristic is not found in all events (cf. Figs. 14-21)

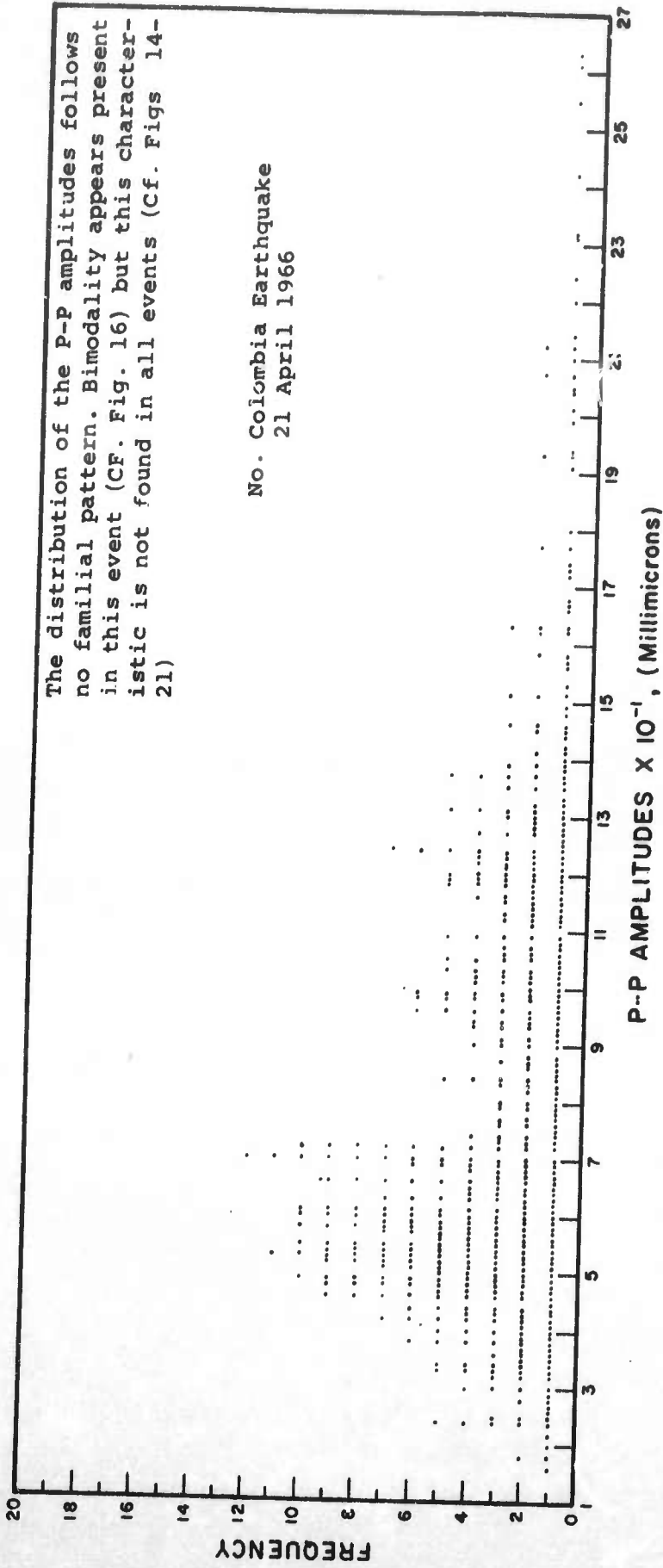


Figure 6. P-P Amplitudes of an Earthquake As Recorded at All LASA SPZ Seismometers.

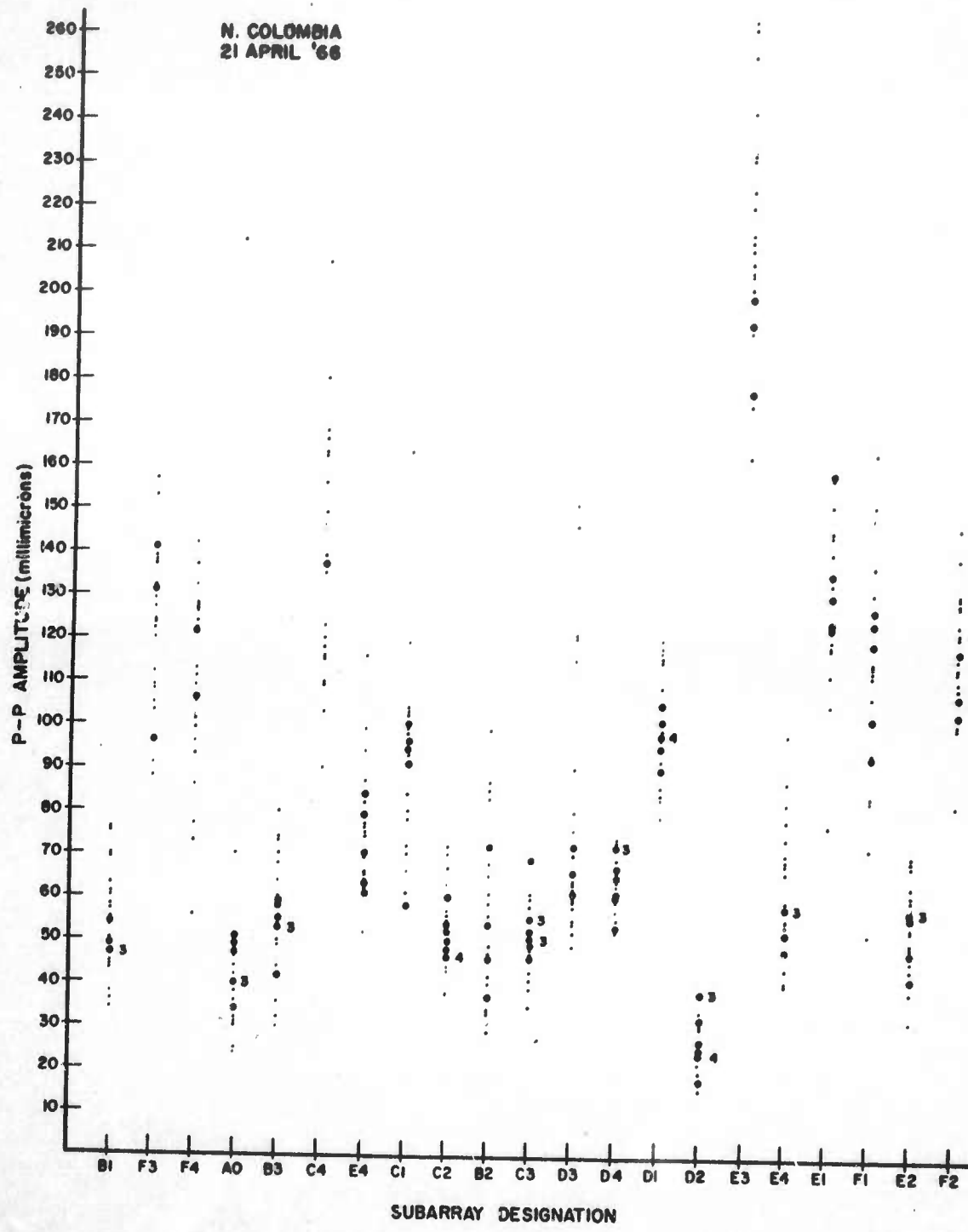


Figure 7. P-P Amplitudes Of An Earthquake
As Recorded At Each Subarray.

occurred at 143° Az with respect to the center of the LASA and ranged from 9,500 km. to 10,500 km. distance. These events were ordered in relation to their distance from the LASA and were partitioned into pairs. The result of this grouping was a set of four pairs of events such that the elements within each pair had epicenters within eight kilometers of each other. Although these epicenters were close together, the focuses of the events had a considerably greater range. Each of the pairs was investigated for the presence of correlation between member events in the following manner. The peak to peak P-phases amplitudes recorded by the center elements of the subarrays were determined for each event. In this way, an ordered set of amplitudes indexed by the recording instruments was associated with each event. Thus, in order to detect the presence of correlation between any two events, one merely tests for correlation between the two sets of amplitudes generated by respective events. But before taking this step, it is important to note that an accurate interpretation of the correlation coefficient is, in general, possible only when the underlying population is normally distributed. It was demonstrated in the discussion under 2, above, that a log-normal distribution describes the behavior of amplitude anomalies over LASA with remarkable precision. Hence, by using the logarithms of the peak to peak amplitudes, each event has been characterized with a normally distributed set of measurements and the correlation theory can now be applied. The estimate of the coefficient of correlation is defined by

$$r = \frac{\text{Cov}(X, Y)}{\sqrt{\text{Var } X \cdot \text{Var } Y}}.$$

Results showed that one pair was correlated, one was borderline, and two were uncorrelated. The pairs were ranked from the highest to the lowest degree of correlation; then the pairs were ranked from those with earthquakes which occurred closest together to those with earthquakes farthest apart. These two rankings yielded the same order in both cases. The events which occurred closest together had the highest correlation and those which occurred farthest apart were least correlated.

Similar tests were performed on three teleseismic events which occurred near the surface, and at the same location. All possible combinations of pairs were tested and in each instance a high positive correlation was found to exist.

C. Radiation of Seismic Waves From the BILBY Explosion

The underground nuclear explosion BILBY was detonated in the Nevada Test site on 13 September 1963. BILBY generated seismic waves which were recorded well at most of the North American stations and

especially at the LRSM stations. Furthermore, it was followed by the cavity collapse (assigned magnitude = 4.5). The presence of this collapse, the relatively large size of the explosion, ($m = 5.8$), radiation of both Rayleigh and Love waves, and the proximity of the site to those of other well recorded explosions such as HAYMAKER and SEDAN have made BILBY ideally suited for a study to determine the mechanism of generation of seismic waves and the radiation pattern.

Because of the particular nature of the desired study and to insure that a procedure of analysis similar to that previously used was exactly followed, it was decided to have Dr. M. Nafi Toksöz, Massachusetts Institute of Technology, conduct this analysis, assisted by Mr. Kevin Clermont, Princeton University.

Basically, the procedures followed were to first minimize the effects of the propagation by determining the radiation patterns of the P-waves and Rayleigh waves of BILBY relative to those of the collapse. Then the ratios of the Love and Rayleigh wave amplitudes were used to determine a source mechanism which was consistent with the Rayleigh wave radiation pattern. The source time function was determined from the amplitude spectra corrected for propagation and instrument effects. Finally, the BILBY results were compared with the HARDHAT, HAYMAKER, SEDAN, and SHOAL explosions. The most significant result is that BILBY, like the HAYMAKER and SHOAL explosions, generated some Love waves. The source mechanism in all cases can be explained in terms of an ideal explosive source superimposed over a tectonic source of double-couple form. The orientation and relative strength of the double-couple seem to be controlled by the properties of the medium and the orientation of the tectonic axis. BILBY (in tuff) and HAYMAKER (in alluvium) were located about 5 km apart. The radiation patterns of Rayleigh waves are almost identical. In both cases the principal plane of the double-couple is oriented in the direction $\theta = 340^\circ$. For the SHOAL explosion, which was detonated in a completely different area, the orientation of the double-couple was in very good agreement with those of earthquakes in the area. These facts suggest that multipolar contributions to the radiation patterns are controlled by the general tectonic features of the region.

D. Synthesis of Additive Ambient Seismic Noise With A Gaussian Markov Model

The purpose of this study was to show that simple synthesized seismic noise models can qualitatively account for many of the observed properties of the noise. Such models are useful for efficiently generating standard test data on a digital computer for checkout of

vertical array processors and for preliminary evaluation and ranking of seismic signal processors.

The ambient seismic noise was modeled by a single Gaussian population from which independent realizations or states were taken as input to tuned filters with spectral peaks matched to those observed in noise samples, for example at .2 cps and 2. cps. For each spectral noise peak, the realization on channel $i + 1$ was equal to a constant times the realization on channel i plus another constant times a new realization on channel $i + 1$. Results showed that the constants defining the Markov process could be used to theoretically derive the associated power spectral matrix of the noise model. The model could be extended to dispersive systems by using a set of constants and time lags to relate the noise on channel i to that on channel $i + 1$.

A vertical array signal model was also given. The purpose was to efficiently generate noise and/or signals at prescribed S/N ratios. The noise covariance structure was close to that observed naturally and was known exactly for the noise model realizations. Thus the spectral covariance of the noise was given exactly, subject only to roundoff error, and conditions of stationarity and equilibrium were satisfied by the data generated for testing and designing multi-channel filters.

E. Principal Component Analysis of Seismic Data

Two technical notes were submitted to the SDL by Measurement Analysis Corporation as part of specialized studies which they performed for the SDL. The work was concerned with the development of the principal component theory to seismic noise records.

Principal component analysis is designed to explain observed relations among sample records obtained from an array of seismometers in terms of simpler relations by reducing the random variables of these records to a small number of linear combinations. The sum of the variances of all principal components is the sum of the variances of the original variables. Thus, if there exist principal components with large variances which account for most of the variability, the dimensionality of the problem might be reduced by attention only to these principal components.

The first note concerned itself with the development of the principal component theory by first summarizing a statistical interpretation of the principal component and then by analysis, based on noise data recorded at the Montana LASA. The analysis consisted of obtaining the proportion of the total variance (power) from 10 seismometers as explained by the first four principal components. Results

showed that at 0.2 cps approximately 80% of the total variance was accounted for by the first principal component.

The second note concerned itself with utilizing the principal component to determine the noise source, based on data from LONGSHOT and a geographically nearby earthquake recorded at a LASA subarray. The phase shifts of the first principal component at 0.2 cps corrected for LASA instrument response resulted in an accurate estimate of the general direction of the main noise source. Computed examples of the data verified this estimate.

F. Eigenvalues and Eigenvectors of Spectral Density Matrices

Measurement Analysis Corporation presented a report which described some interpretations and uses of eigenvalues and eigenvectors of spectral and sample spectral density matrices of multiple stationary time series.

The spectral density matrix of a zero-mean multiple stationary time series was defined. Eigenvalues and eigenvectors of the spectral density matrix were discussed and principal component theory was presented. Statistical distribution theory and related results were used to investigate the eigenvalues of a sample spectral density matrix. This investigation gave methods for obtaining simultaneous confidence bounds on the elements of the true spectral density matrix and its inverse, and also methods for obtaining confidence bounds on the eigenvalues of the true spectral density matrix.

G. Shot and Earthquake Analyses

Standard statistical summary reports were issued on the Nevada Test Site nuclear events BOURBON, NASH, and GREELEY. Table 2 summarizes part of the seismic data compiled from these analyses.

Other projects completed included photo albums from four events and travel-time computations for NTS and other sites.

Event Name	Event Date	Medium	Magnitude	No. of Stations Recording	
				SP Signals	LP Signals
BOURBON	20 January 1967	Tuff	5.09 ± 0.61	15	15
NASH	19 January 1967	Tuff	5.25 ± 0.50	15	8
GREELEY	20 December 1966	Zeolitized Tuff	6.29 ± 0.45	25	26

Table 2. Seismic Data From Three Nuclear Explosions

III. SUPPORT AND SERVICE TASKS

A. VELA-UNIFORM Data Services

As part of the contract work-statement, the SDL provided one or more of the following support and service functions for VSC and other VELA participants:

- copies of 16 and 35 mm film
- playouts of earthquakes and special events
- copies of existing composite analog tapes
- composite analog tapes of special events
- use of 1604 computer for checking out new programs or running production programs
- copies of digital programs
- digitized data in standard formats or special formats for use on computers other than the 1604
- running SDL production programs, such as power spectral density and array processing of specified data
- digital x-y plots of power spectra or digitized data
- signal reproduction booklets
- copies of MIT Geophysics Program Set II
- space for visiting scientists utilizing SDL facilities to study data and exchange information with SDL personnel.

During this report period, 51 such projects were completed and the 15 organizations receiving these services are listed in Appendix A.

B. Data Library

The Data Library contains approximately 7,000 digitized seismograms, 170 digital computer programs and 290 composite analog magnetic tapes, all available for use by the VELA-UNIFORM program.

The following additions were made during this period.

1. Digital Seismograms - 372 including
 - data from 10 explosions and 3 underwater events
 - noise samples from LASA, TFO, UBSO, CPSO, and WMSO
 - noise from several vertical arrays
 - earthquake data recorded at various stations
2. LASA Data - 84 digital tapes
 - there are a total of 785 digital tapes in the library. There is also a master calibration tape which contains the magnification (digital counts per millimicron) of each sensor for every subarray. These magnifications have

been computed for all calibration tapes currently in house. As each new calibration is received, it is routinely run through the program CALIBR and added to the master tape.

3. Digital Programs - 19 including:

ARCTANGENT FUNCTION - to compute the arctangent of the ratio X/Y, based on certain conditions.

CALIBR - to compute the magnification level (counts per millimicron) of each LASA seismometer

PARDATA - to take an input tape containing a label and i no. of data traces X_i , partition X_i into j no. of data traces X_{ij} , and write a new tape containing either a/or no. label and $X_{i1}, X_{i2}, \dots, X_{ij}$

RELABLIB - using standard FORTRAN-63 library seismogram tapes, either the packed or unpacked format, this program will relabel seismograms, copy seismograms, skip seismograms, merge tapes, or any combination of these operations.

SPECMAT - to compute the theoretical power spectral density matrix for the Gaussian Markov model.

SPECMTRX - to compute theoretical power spectral densities, coherencies, and phases for the Gaussian Markov chain.

LOPER - to reformat the long period multiplexed digital LASA data which were recorded at 5 points per second on the slow mode tapes into standard SDL library tape format.

SHOPER - to reformat the short period multiplexed digital LASA data which were recorded at 20 points per second on the slow mode tapes into standard SDL library format.

FORDEC - to read a standard SDL library tape whose sampling rate is 20 samples per second and decimate the data to 10 samples per second and write it onto a tape in standard SDL library format with corrections in the label of the new tape for sampling rate and number of points.

RMS ONLY - to read up to 9 seismograms from a magnetic tape, in subset tape format, detrend, filter (optional), compute rms on a particular desired region, and the mean of the rms.

LOPDEC - to reformat the long period multiplexed digital LASA tapes which were recorded at 5 points per second into standard SDL library tapes decimated to 1 point per second.

SPECSUB - to read up to 6000 points of data in sub-set format, detrend, demagnify, filter it and form a new sub-set tape.

LASAN - to read fast mode LASA data, 20 samples per second, less than 3000 points, from a standard SDL library tape and further process the data.

ALAST - ALAST reads the save tapes prepared by MODLAS or LASAN and aligns the traces according to the Delta T's and Anomalies supplied by the user and makes a new save tape with traces aligned and in sub-set format.

MODLAS - to read LASA data from an SDL library tape and further process data.

LOPSAN - LOPSAN is a 1604 program designed to read LP data from SDL library format tapes whose sampling rates are 1 to 5 samples per second, up to 12000 points, and further process the data.

PREDICT - to compute a prediction of the straight sum of Multi-channel arrays, ispan units ahead in time where ispan is the prediction span. The predicted sum and the actual sum are subtracted to yield a prediction error, and all are plotted to the same scale factor. Also, to compute and plot power-spectra of these traces.

VFKSPTRM - to compute and display the frequency-wave number power spectra of seismic noise along with a response function for the corresponding vertical array.

AMBILOG - to convert a Geotech Ambilog digital tape into the standard SDL unpacked library tape format and produce a seismogram label listing and punched index cards.

4. Analog Composite Tapes - 10 including:

a. Made by SDL

- OONW data for Lincoln Laboratory
- Earthquake data for USCGS

b. Made by Geotech

- PERSIMMON
- AGILE

C. Data Compression

This is a continuing routine operation, and production is maintained at the level needed to meet the requirements of the field operation (LRSM and U. S. Observatories) and the Seismic Data Laboratory. For this period, 1,244 tapes were compressed.

D. Automated Bulletin Process

January, February, and March 1967 LRSM and Observatory bulletins were processed during this report period and forwarded to the Geotech, A Teledyne Company, for checking and publication.

APPENDIX A

ORGANIZATIONS RECEIVING SDL DATA SERVICES

April - June 1967

Colorado School of Mines

Earth Sciences, Teledyne

General Atronics Corporation

Geotech, Teledyne

IBM Corporation

Lamont Geophysical Observatory

Massachusetts Institute of Technology

Oregon State University

Pennsylvania State University

Princeton University

San Calixto, Bolivia, Observatory

Texas Instruments, Incorporated

University of California

University of Michigan

U. S. Coast and Geodetic Survey

Unclassified

Security Classification

DOCUMENT CONTROL DATA - R&D

(Security classification of title, body of abstract and indexing annotation must be entered when the overall report is classified)

1. ORIGINATING ACTIVITY (Corporate author)	2a. REPORT SECURITY CLASSIFICATION Unclassified
TELEDYNE, INC. ALEXANDRIA, VIRGINIA 22314	2b. GROUP ---

3. REPORT TITLE

SEISMIC DATA LABORATORY QUARTERLY TECHNICAL SUMMARY REPORT

4. DESCRIPTIVE NOTES (Type of report and inclusive dates)

Quarterly Summary - April - June 1967

5. AUTHOR(S) (Last name, first name, initial)

Dean, William C.

6. REPORT DATE 17 July 1967	7a. TOTAL NO. OF PAGES 26	7b. NO. OF REFS
8a. CONTRACT OR GRANT NO. F 33657-67-C-1313	8a. ORIGINATOR'S REPORT NUMBER(S)	
8b. PROJECT NO. VELA T/6702		
c. ARPA Order 624	8b. OTHER REPORT NO(S) (Any other numbers that may be assigned this report)	
d. ARPA Program Code No. 5810	Technical Summary Report No. 16	
10. AVAILABILITY/LIMITATION NOTICES This document is subject to special export controls and each transmittal to foreign governments or foreign national may be made only with prior approval of Chief, AFTAC.		
11. SUPPLEMENTARY NOTES ---	12. SPONSORING MILITARY ACTIVITY ADVANCED RESEARCH PROJECTS AGENCY NUCLEAR TEST DETECTION OFFICE WASHINGTON, D. C.	

13. ABSTRACT

This report discusses the work performed by SDL for the period April through June 1967, and is primarily concerned with seismic research activities leading to the detection and identification of nuclear explosions as distinguished from earthquake phenomenon. Also discussed are the data services performed for other participants in the VELA-UNIFORM project.

DD FORM 1 JAN 68 1473

Unclassified
Security Classification

Unclassified
Security Classification

14. KEY WORDS	LINK A		LINK B		LINK C	
	ROLE	WT	ROLE	WT	ROLE	WT
Seismic Data Laboratory - Quarterly Technical Summary VEIA-UNIFORM Project Seismic Data Analysis Large Aperture Seismic Array Seismic Noise Principal Components of Seismic Noise Coherency Analyses						
INSTRUCTIONS						
1. ORIGINATING ACTIVITY: Enter the name and address of the contractor, subcontractor, grantee, Department of Defense activity or other organization (corporate author) issuing the report.	imposed by security classification, using standard statements such as:					
2a. REPORT SECURITY CLASSIFICATION: Enter the overall security classification of the report. Indicate whether "Restricted Data" is included. Marking is to be in accordance with appropriate security regulations.	(1) "Qualified requesters may obtain copies of this report from DDC."					
2b. GROUP: Automatic downgrading is specified in DoD Directive 5200.10 and Armed Forces Industrial Manual. Enter the group number. Also, when applicable, show that optional markings have been used for Group 3 and Group 4 as authorized.	(2) "Foreign announcement and dissemination of this report by DDC is not authorized."					
3. REPORT TITLE: Enter the complete report title in all capital letters. Titles in all cases should be unclassified. If a meaningful title cannot be selected without classification, show title classification in all capitals in parenthesis immediately following the title.	(3) "U. S. Government agencies may obtain copies of this report directly from DDC. Other qualified DDC users shall request through _____."					
4. DESCRIPTIVE NOTES: If appropriate, enter the type of report, e.g., interim, progress, summary, annual, or final. Give the inclusive dates when a specific reporting period is covered.	(4) "U. S. military agencies may obtain copies of this report directly from DDC. Other qualified users shall request through _____."					
5. AUTHOR(S): Enter the name(s) of author(s) as shown on or in the report. Enter last name, first name, middle initial. If military, show rank and branch of service. The name of the principal author is an absolute minimum requirement.	(5) "All distribution of this report is controlled. Qualified DDC users shall request through _____."					
6. REPORT DATE: Enter the date of the report as day, month, year; or month, year. If more than one date appears on the report, use date of publication.	If the report has been furnished to the Office of Technical Services, Department of Commerce, for sale to the public, indicate this fact and enter the price, if known.					
7a. TOTAL NUMBER OF PAGES: The total page count should follow normal pagination procedures, i.e., enter the number of pages containing information.	11. SUPPLEMENTARY NOTES: Use for additional explanatory notes.					
7b. NUMBER OF REFERENCES: Enter the total number of references cited in the report.	12. SPONSORING MILITARY ACTIVITY: Enter the name of the departmental project office or laboratory sponsoring (paying for) the research and development. Include address.					
8a. CONTRACT OR GRANT NUMBER: If appropriate, enter the applicable number of the contract or grant under which the report was written.	13. ABSTRACT: Enter an abstract giving a brief and factual summary of the document indicative of the report, even though it may also appear elsewhere in the body of the technical report. If additional space is required, a continuation sheet shall be attached.					
8b, 8c, & 8d. PROJECT NUMBER: Enter the appropriate military department identification, such as project number, subproject number, system numbers, task number, etc.	It is highly desirable that the abstract of classified reports be unclassified. Each paragraph of the abstract shall end with an indication of the military security classification of the information in that paragraph, represented as (TS), (S), (C), or (U).					
9a. ORIGINATOR'S REPORT NUMBER(S): Enter the official report number by which the document will be identified and controlled by the originating activity. This number must be unique to this report.	There is no limitation on the length of the abstract. However, the suggested length is from 150 to 225 words.					
9b. OTHER REPORT NUMBER(S): If the report has been assigned any other report numbers (either by the originator or by the sponsor), also enter this number(s).	14. KEY WORDS: Key words are technically meaningful terms or short phrases that characterize a report and may be used as index entries for cataloging the report. Key words must be selected so that no security classification is required. Identifiers, such as equipment model designation, trade name, military project code name, geographic location, may be used as key words but will be followed by an indication of technical context. The assignment of links, rules, and weights is optional.					
10. AVAILABILITY/LIMITATION NOTICES: Enter any limitations on further dissemination of the report, other than those						